

Vibrational Spectra and Conformations of Chloro- and Bromo-cyclobutane

A. Gatial, P. Klæboe, C. J. Nielsen, D. L. Powell and D. Sülzle

Department of Chemistry, University of Oslo, BOX 1033, 0315 Oslo 3, Norway

A. J. Kondow

Department of Chemistry, The College of Wooster, Wooster, Ohio 44691, USA

The Raman and IR spectra of chloro- and bromo-cyclobutane as vapours, liquids and as amorphous and crystalline solids were recorded at various temperatures. Additional IR spectra of the high-pressure crystalline phases were obtained at ca 25 kbar pressure. IR matrix isolation spectra were recorded at 14 K, using the hot nozzle technique.

Evidence is presented to show that chloro- and bromo-cyclobutane have a second (axial) conformer existing in amounts less than 10% for chloro- and 3% for bromo-cyclobutane at ambient temperature, in addition to the dominant (equatorial) conformer. From the study of the Raman spectra of the liquid and vapour as a function of temperature, enthalpy differences between the two conformers were calculated. The axial conformers could not be trapped at 17 K, revealing the barrier to ring conversion to be smaller than 5 kJ mol⁻¹.

New vibrational assignments, supported by normal coordinate analyses are presented for both compounds.

INTRODUCTION

For the past 20 years, the question of whether mono-substituted cyclobutanes can exist, in any appreciable amounts, in axial conformations has been an open one. Although Rothschild¹ postulated second (axial) conformers on the basis of infrared and Raman studies of chlorocyclobutane and bromocyclobutane, an interpretation which the work of Durig and co-workers^{2,3} tended to support, further evidence in support of the existence of these conformers has not been easily forthcoming. Far-infrared studies⁴ on chloro-, bromo- and cyano-cyclobutane all suggest either a single conformer (bromo- and cyano-cyclobutane) or a second conformer of energy much greater than the equatorial (chlorocyclobutane), although the Raman data for bromocyclobutane have also been interpreted in terms of two minima with a large energy difference between them.⁵

In earlier microwave work on chlorocyclobutane,⁶ bromocyclobutane⁷ and cyanocyclobutane,^{8,9} the equatorial conformer alone was detected in each case. However, very recent structural work on cyanocyclobutane has led to the postulation of an axial conformer 3.1 kJ mol⁻¹ above the equatorial.¹⁰ In addition, recent electron diffraction studies of chloro and bromocyclobutane by Jonvik¹¹ led to the conclusion that axial and equatorial conformers exist for both over the temperature range employed (290–700 K). In both compounds the best fit to the data was found with a barrier height larger than 1.5 kJ mol⁻¹. From the results of *ab initio* calculations, it was concluded¹² that an axial conformer exists in chlorocyclobutane with energy 4.3 kJ mol⁻¹ above the equatorial.

In contrast, the situation has been much clearer for several other cyclobutanes with a single substituent group XH₃, where X = C, Si or Ge. In these com-

pounds both axial and equatorial conformers have been found in substantial amounts.^{13–16}

A fuller discussion of the relevant background appears in a review by Legon,¹⁷ whereas Allen¹⁸ has reviewed the geometry of cyclobutanes in the crystalline phase.

Our own work on 1,1,2-trichloro-2,3,3-trifluorocyclobutane¹⁹ convinced us that it might indeed be possible to find, in a favourable case, convincing evidence for an axial conformer in a monosubstituted cyclobutane. In this paper we report our results for chlorocyclobutane and bromocyclobutane; cyanocyclobutane will be discussed in a paper to follow.

EXPERIMENTAL

The samples used were obtained from Fairfield Chemical and were purified by preparative gas chromatography.

Infrared spectra were recorded on a Perkin-Elmer Model 283 spectrometer, a Perkin-Elmer Model 225 spectrometer and a Bruker IFS-114c evacuable fast-scan Fourier transform spectrometer. Spectra were taken of the compounds as liquids and as unannealed and annealed solids at both low temperature and high pressure. For the high-pressure spectra a diamond anvil cell from High Pressure Diamond Optics and a Perkin-Elmer 4 × beam condenser were employed.

Spectra were also recorded of the compounds isolated in argon and nitrogen matrices on a CsI window in a Displex unit from Air Products. Using a heated quartz nozzle, samples were deposited not only from a 1000:1 mixture of gas at room temperature, but also at temperatures up to 900 K for chlorocyclobutane and 700 K for bromocyclobutane. The temperature of the window was 17 K during deposition and 13 K during recording

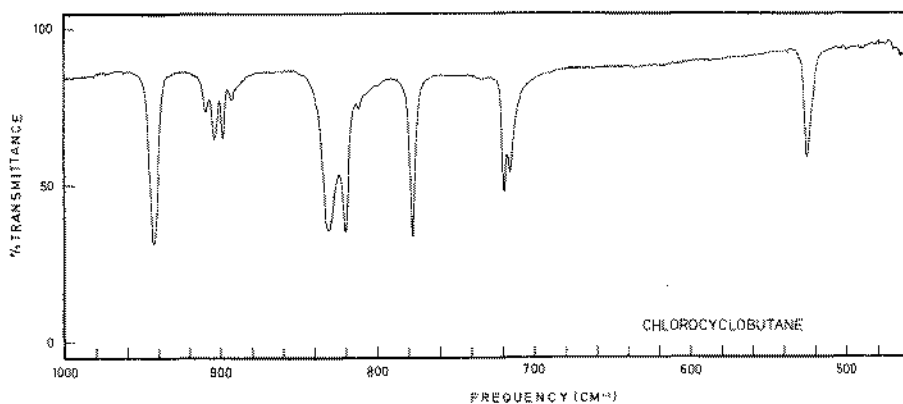


Figure 1. Infrared spectrum of chlorocyclobutane as a crystalline solid at 90 K.

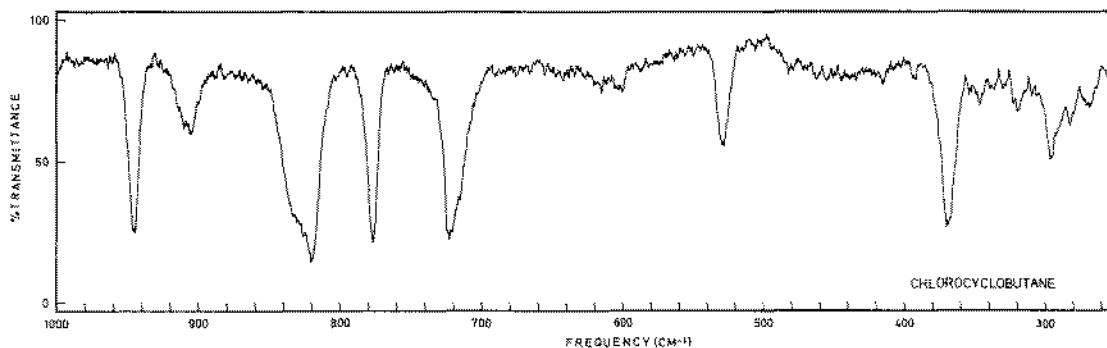


Figure 2. Infrared spectrum of chlorocyclobutane as a high-pressure crystal at 25 kbar.

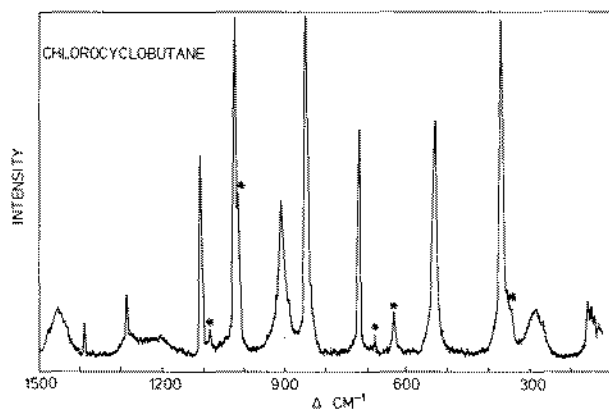


Figure 3. Raman spectrum of chlorocyclobutane vapour; the asterisks denote axial conformer bands.

of spectra. No decomposition products were detected at any time.

Raman spectra were recorded of the vapours, liquids and annealed crystalline solids and of the liquids at different temperatures in a capillary tube of 2 mm i.d. surrounded by a Dewar vessel and cooled with gaseous nitrogen.²⁰ These were done using a Dilor RT 35 spectrometer (triple monochromator) interfaced to the Aspect 2000 data system of the Bruker FTIR instrument and excited by the 514.8 nm line of a Spectra-Physics Model 2000 argon ion laser.

RESULTS AND DISCUSSION

Portions of the low-temperature and high-pressure IR spectra of chlorocyclobutane as a crystalline solid are shown in Figs 1 and 2. A Raman spectrum of the vapour is given in Fig. 3 and detailed spectra of the liquid at various temperatures are shown in Fig. 4. A Raman spectrum of the crystalline solid is presented in Fig. 5 and an IR spectrum of the compound isolated in an argon matrix is given in Fig. 6. To save space, only those results new in this study are shown in Table 1.

An infrared crystal spectrum of bromocyclobutane in the 1000–400 cm^{-1} region, recorded at 90 K, is shown in Fig. 7. Small portions of the Raman spectra of the liquid at various temperatures are given in Figs 8 and 9, a crystal spectrum is shown in Fig. 10. The experimental data are listed in Table 2.

Inclusion compounds

The formation of an inclusion compound of mono- and di-substituted cyclohexanes has been shown to shift the equatorial-axial equilibrium toward the axial conformer.²¹ In the cyclobutanes we hoped that a similar shift might occur so that we could detect an axial conformer. Unfortunately, no clathrates were formed with either urea or thiourea. This was not wholly unexpected

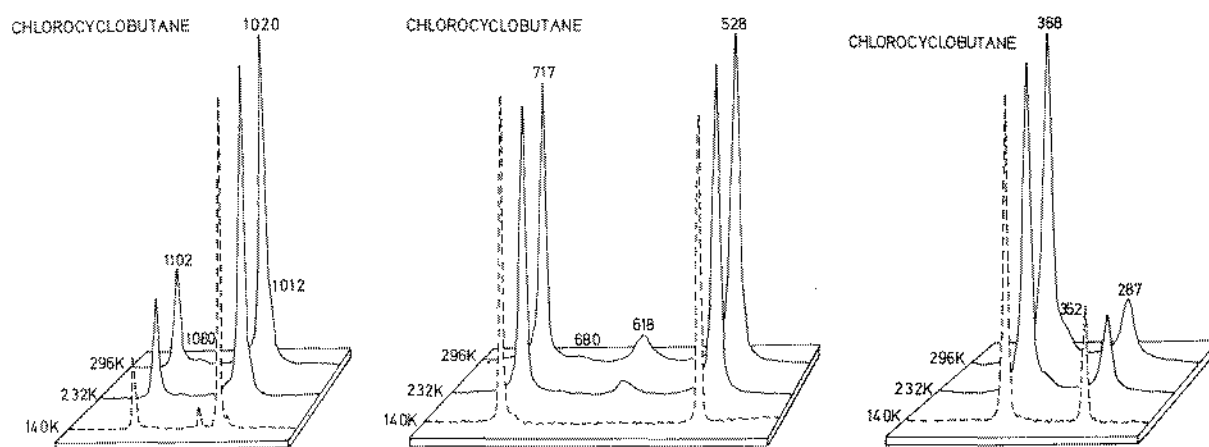


Figure 4. Raman curves of significant regions of chlorocyclobutane. Solid lines, liquid at 296 and 232 K; dashed line, crystalline solid at 140 K.

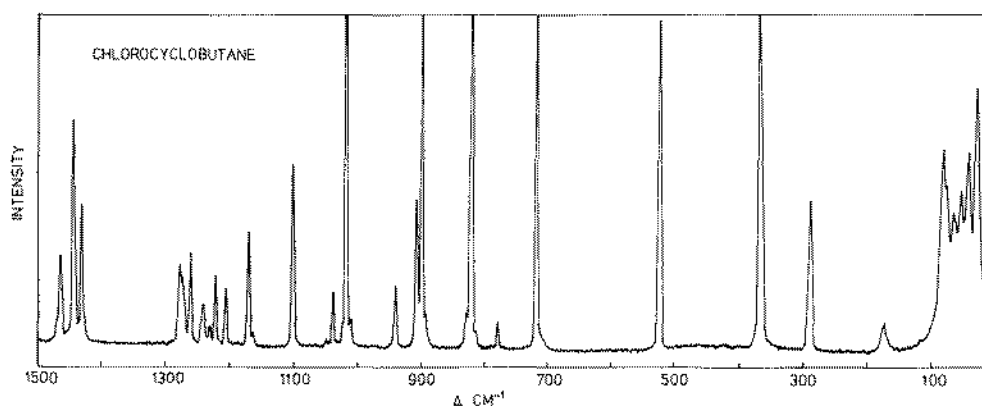


Figure 5. Raman spectrum of crystalline chlorocyclobutane at 140 K.

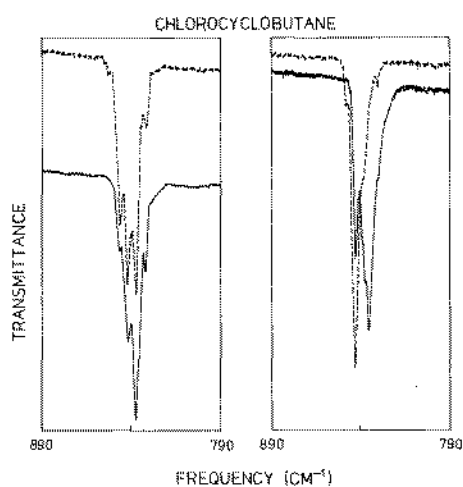


Figure 6. Infrared curves of chlorocyclobutane in the region 890–790 cm^{-1} , matrix isolated in argon (left) and in nitrogen (right) at 14 K (nozzle temperature 312 K). Top curves, before annealing; bottom curves, annealed at 34 K for 50 min.

as the cyclobutanes may be too large for urea and too small to form inclusion compounds with thiourea.

Matrix spectra

In the matrix experiments our primary goal was to see if any bands due to a second conformer could be seen in the spectra of the sample deposited from a hot nozzle. We found that the spectra of the sample deposited at elevated temperatures were essentially identical with those taken at room temperature. From this we can conclude that either the (presumed) second conformer lies more than 22 kJ mol^{-1} above the first (assuming an abundance of at least 5% at 900 K is required to be detectable) or that the barrier between the two conformers is so low ($< 5 \text{ kJ mol}^{-1}$) that conversion at 17 K occurs so rapidly that the unstable form is not seen.

Even after annealing for 30 m at 35 K, many of the bands due to fundamentals have one or more near-lying neighbours. In several cases, a weak band is present in one matrix but not in the other, thus establishing it as

Table 1. Infrared and Raman spectral data for chlorocyclobutane^a

Vapour	Infrared				Raman			Assignment
	Ar matrix (14 K)	N ₂ matrix (14 K)	Liquid	Solid crystal 90 K	Vapour	Liquid (150 K)	Solid crystal (90 K)	
3008								
3003	-s, A	3016 m	3006 s	2996 s	2996 s	2998 w, sh	2997 m	ν_1
2997		3007 w			2986		2987	
2988	-s, A	2997 m	2996 mw	2986 s		2983 s, P	2983	ν_2
2980			2989 mw		2981			
2977								
2974c	-s, B	2988 w	2981 vw			2973 w, sh	2973 ms	ν_{19}
2971								
		2966 w	2973 vw					ν_{20}
2967		2960 w, sh	2966 m					
2962	-s, A	2956 s	2962 m	2950 vs	2951 vs	2956 vs, P	2953 vs	ν_3
2957		2952 w, sh	2957 w, sh		2948 w, sh			
					2927 vvw		2930 vvw	$2 \times \nu_6$
2941								
2935	-m, A	2933 vw	2934 w	2925 vs	2918 w	2925 s, P	2920 s	ν_4
2928								
		2902 w	2904 w					$2 \times \nu_7$
		2895 vvw	2894 vw					
2901								
2893	-w, A	2885 vw	2885 vvw	2896 s	2887 m	2883 w, P	2884 vw	ν_5
2885								
		2873 w, sh	2878 vw		2876 vw	2871 w, P?		$\nu_7 + \nu_{21}$
		2870 mw	2873 w					
2882								
2875c	-w, B	2860 vw	2865 vw	2856 s	2860 m	2858 m, P?	2862 w	$\nu_{20}?$
2870								
					2849 w		2852 m	$2 \times \nu_{21}$
					2838 vvw			
1484								
1478	-w, A	1473 w	1474 w	1468 m	1464 mw	1478 w, sh	1465 w	ν_8
1473								
1462		1452 vvw↓	1453 mw		1450 vvw			
1454	-m, A	1448 mw↑	1447 w	1445 m	1442 m	1455 w	1444 m	ν_7
1446								
1444		1438	1440					
1441c	-w, B			1434 ms	1431 s	1440 w, sh	1435 w	ν_{21}
1436		1437	1438					
			1436 vw, sh		1426 w, sh			$2 \times \nu_{15}$
				1377 w	1382 vvw	1389 mw		$\nu_{12} + \nu_{17}$
					1343 vw			$\nu_{11} + \nu_{30}$
					1322 vvw			$\nu_{14} + \nu_{16}$
1292								
1286	-vs, A	1285 vs	1287 vs	1279 vs	1283 s	1287 m	1281 m, P	ν_8
1279		1282 w, sh	1285 w, sh					
		1273 vvw	1278 w, sh					
		1269 vvw	1275 vvw	1270 s, sh	1273 w, sh		1274 w, sh	
		1265 vvw↓	1263 vw		1264			
1264 w, sh		1263 w↑	1260 mw	1259 m		1260 w, D	1261 m	ν_{22}
		1260 vvw↓			1260			
1255 w		1251 vvw	1250 vvw		1248 m			$\nu_{15} + \nu_{16}$
		1249 vvw						
1242 vvw								
1241 vvw								
1239 w		1238 mw	1239 mw	1236 m	1236 m	1237 vvw	1238 w, D	ν_{23}
1227 vvw?		1229 vw	1227 vvw?		1230 m		1227 vw, P	ν_9
				1225 w, br				
1222 vvw?		1220 vw?	1221 vw		1222 m		1219 vw, D	ν_{24}
1212								
1206	-w	1203 w	1207 w	1200 m	1206 ms	1206 vvw	1204 m, P	ν_{10}
1198			1205 vw, sh					
1171					1171			
1164c	-vw, B	1167 vw	1164 vw	1162 w			1166 m, D	ν_{25}
1157					1165		1165 w, sh	
1106 vw, A		1103 vvw	1104 vvw	1101 vw	1101 w	1105 s	1102 s, P	ν_{11}

Table 1. continued

		Infrared			Raman		Assignment	
Vapour	Ar matrix (14 K)	N ₂ matrix (14 K)	Liquid	Solid crystal 90 K	Vapour	Liquid (150 K)	Solid crystal (90 K)	
1081 vw, A				*	1080 w†	1080 w, P†	*	ν'_{11} $2 \times \nu_{16}$
	1050 vvw	1058 vvw 1046 vvw?		1047 w 1042 vw			1050 vvw	
	1032 vw	1032 vw	1035 w	1035 w	1031 vvw	1034 w, D	1039 w	ν_{26}
1029	1023 m↓							
1024	1021 m↓	1025 w, sh		1019 w, sh				
1022 } s, A	1019 vs†	1022 vs	1018 vs	1017 vs	1023 vs	1020 vs, P	1021 vs	ν_{12}
1020	1017 w, sh	1020 w, sh		1014 w, sh				
1015								
1012 w, sh			1010 w, sh	*	1014 m†	1012 w, P†	*	ν'_{12}
1005 w, sh	1011 vvw	1013 vvw		1010 w 1000 w, sh			1012 w, sh	$\nu_{16} + \nu_{30}$
944								
938c } vw, B	943 w†	942 w†	939 m	942 m		942 w, D	942 w	ν_{27}
931	938 vw↓	938 mw↓						
912 w, sh	906 vw	908 vw		909 vvw		906 m, P?	909 m	ν_{13}
			903 m		907 m, brd			
906				903 mw				
902 } w, B?	902 w	904 vvw		897 w		902 s, D?	901 vs	ν_{28}
	899 vw	900 vw		892 vw 884 vvw			894 vw, sh	$\nu_{16} + \nu_{17}$ $\nu_{15} + \nu_{18}$
856	852 vw↓							
850	846 m↓	848 w↓						
846 } vs, A	842 s↓	843 vs↓	832 vs	826 s	849 s	828 s, P	830 vw, sh 822 s	ν_{14}
842	837 s†	838 w, sh†						
	832 w†	830 vw†						
				819 m, sh 811 w, sh			814 vvw	$\nu_{16} + \nu_{30}$
789								
781c } vw, B	780 vvw	783 vw	779 vw	777 s		782 vw, D	780 vw	ν_{29}
776	775 vvw							
724	721 m↓	726 vw↓		719 w, sh				
717 } s, A	716 s†	720 s	716 s	713 s	718 s	717 s, P	718 s	ν_{15}
710				706 w, sh			705 vw, sh	
685								
677 } vw, A			678 w	*	678 vw†	680 vw, P†	*	ν'_{15}
668								
636								
630 } vw, A			616 m	*	630 w†	618 w, P†	*	ν'_{16}
626								
538	533 w↓							
534	530 mw↓	530 m↓						
530 } m, A	528 m†	527 w, sh†	528 s	524 s	531 s	528 s, P	525 s	ν_{16}
526	525 vw, sh	524 vw†		520 w, sh				
524								
376	371 vw, sh	371 mw↓						
370 } m, A	366 mw	368 w†	366 s	367 s	370 s	368 s, P	370 s	ν_{17}
364	363 vw, sh			363 m, sh				
355 w			352 w, sh	*	351 w, sh	352 w, P†	*	ν'_{17}
289	290 vw	289 vvw						
283c } vw, B	287 w	285 w	284 w	293 m 284 w 280 vw	287 w	287 m, D	291 m	ν_{30}
277	281 vw							
					156 w 149 w 139 w 129 vw	162 vw, P	174 vw	ν_{18}
							80 m	l.m.
							55 mw	l.m.
							45 m	l.m.
							31 m	l.m.

^a Abbreviations: s, strong; m, medium; w, weak; v, very; sh, shoulder; c, central; brd, broad; P, polarized; D, depolarized. A, B and C denote vapour contours. Arrows (↓ or †) in matrix spectra denote bands which decrease or increase in intensity after annealing and in Raman spectra (†) denote bands enhanced at higher temperatures. Asterisks signify bands vanishing in the crystal spectra and believed to be due to an unstable conformer.

Table 2. Infrared and Raman spectral data for bromocyclobutane^a

Vapour	Infrared				Raman		Assignment	
	Ar matrix (14 K)	N ₂ matrix (14 K)	Liquid ^b	Solid crystal 90 K	Liquid (150 K)	Solid crystal (80 K)		
3010		3015 m, sh						
3004 }-s, A	3021 m	3010 s-	2995 vs	2992 s	2996 m, P	2994 m	ν_1	
2996	3003 w, sh	3007 s-						
2988 }-s, A	2997 s	2992 m	2987 w, sh	2980 s	2983 s, P	2980 s	ν_2	
2982	2988 w, sh							
	2982 m	2982 w			2971 w, D?	2971 m	ν_{19}	
	2968 w	2970 w			2962 vw, D?	2960 vw, sh	ν_{20}	
2966	2958 w, sh			2950 w, sh		2954 w, sh		
2961 }-s, A	2954 s	2958 m	2949 vs	2945 vs	2948 vs, P	2945 vs	ν_3	
2956	2950 w, sh	2948 w, sh						
2938 vw, sh	2939 w, sh	2938 w, sh		2933 w, sh	2938 w, sh	2938 w, sh	$2 \times \nu_6$	
2925 vw	2923 w	2924 vw	2917 w, sh	2905 w	2910 m, P	2906 m	ν_4	
	2898 w	2900 w	2892 w, sh	2884 vw	2889 w, D?	2888 vw	$2 \times \nu_7$	
2893								
2887 }-w, A	2882 mw	2884 mw	2874 m	2862 m	2870 w, P	2864 w	ν_5	
2881	2877 w, sh	2878 w, sh						
2875 vw, sh	2866 w	2868 w	2863 w, sh	2855 w	2850 w, P	2848 w	$2 \times \nu_{21}$ $\nu_{20}?$	
				2846 vw				
1476								
1472 }-w, A	1466 w	1466 w	1459 w, sh	1458 w	~ 1470 vw	1461 w, P	1458 w	ν_6
1468		1463 vw, sh						
1457	1452 vw↓			1441 w, sh				
1452 }-m, C	1447 m↑	1448 m	1442 m	1438 m	1449 w	1443 m, P	1443 m	ν_7
1446							1439 vw, sh	
1445								
1440c }-w, B	1440 mw	1440 m	1434 w, sh	1433 s	~ 1440 vw	1435 w, D	1434 w	ν_{21}
1435								
	1424 vvw	1424 vvw		1424 vw		1427 w, sh	1425 vw, sh	$\nu_{16} + \nu_{27}$
					1389 mw	~ 1395 vvw	~ 1400 vvw	$\nu_{17} + \nu_{11}$ $2 \times \nu_{15}$ $\nu_{16} + \nu_{13}$
						~ 1375 vw	~ 1371 vvw	$\nu_{16} + \nu_{28}$ $\nu_{17} + \nu_{12}$ $\nu_{16} + \nu_{14}$
					1321 vvw			$\nu_{17} + \nu_{12}$
					1295 vvw			$\nu_{16} + \nu_{14}$
1282 vw, sh	1282 vw	1285 vw		1270 w	1288 w	1272 vw, D?	1270 vw, sh	ν_{22}
1267	1270 w	1272 w		1263			1260 vw, sh	
1262 }-vs, A	1260 vs	1262↓	1254 vs	1253	1262 m	1254 m, P	1255 m	ν_8
1257		1259↓		1253				
1239	1237 vw↓	1238 vw↑		1236				
1234 }-w, A?	1234 m↑	1234 mw↓	1230 w, sh	1232	1234 w	1232 w, P	1233 mw	ν_9
1230				1226 mw				
	1226 vw	1228 vvw		1226 mw		1226 vw, D?	1226 vw	ν_{23}
~ 1225 vvw?	1220 vw↓		1215 w, sh	1220 mw		1219 vw, D?	1220 w	ν_{24}
	1217 vw↑	1220 w						$\nu_{17} + \nu_{13}$
	1212 vvw	1214 vvw						
		1208 vvw						
1202	1200 m↑	1202 w, sh↓		1202 vw				
1198 }-m, A	1196 m↓	1199 m↓	1192 m	1193 m	1204 vvw?	1195 w, P	1195 w	ν_{10}
1194	1193 m↑	1196 m↑						
	1184 vw	1187 vw	1181 w	1183 vw	1184 vvw?		1183 vw, sh	$\nu_{16} + \nu_{15}$
1165								
1159c }-vw, B	1164 m↑	1164 w↑	1159 vw	1166 w	1154 vvw?	1161 w, D	1166 w	ν_{25}
1154	1160 vvw↓	1161 w↓		1160 w			1159 vw, sh	
1097	1091 vw↓	1092 mw↓						
1092 }-vw, A	1088 m↑	1088 mw↑	1086 w	1089 mw	1091 m	1090 m, P	1090 mw	ν_{11}
1086								
	1028 vw	1029 vw		1030 vw	1063 w↑	1061 w, P↑	*	ν'_{11}
						1029 w, D	1034 w	ν_{26}
							1030 vw, sh	
1021	1022 vw↓	1020 w↓						
	1018 w↓	1017 s↓		1015 w, sh				
1016 }-s, A	1014 vs↑	1016 s↑	1013 m	1013 vs	1016 s	1016 s, P	1016 s	ν_{12}
	1011 w↓	1007 vvw↓						
1011	1008 vw↓							
			1001 w, sh	*	1006 m↑	1005 w, P↑	*	ν'_{12}
	1005 vvw			1005 vw			1007 vw, sh	$\nu_{17} + \nu_{15}$
	994 vvw	996 vvw					1001 vvw	
966 vvw	964 vvw	968 vvw			~ 972 vvw	~ 967 vvw		$2 \times \nu_{16}$
944								
938c }-vw, B	942 mw	941 w↑	937 w	942 m		942 w, D	940 w	ν_{27}
930		937 w↓						
	923 vw			905 w		908 m, P?	905 m	ν_{13}
	921 w	924 w		901 w				

Table 2. continued

Vapour	Infrared				Vapour	Raman		Assignment
	Ar matrix (14 K)	N ₂ matrix (14 K)	Liquid	Solid crystal 90 K		Liquid (150 K)	Solid crystal (90 K)	
~902 vvw?			898 w		900 m, brd			
	902 vw, sh 898 vw 896 vw	910 vvw↓ 904 vw↑ 899 vvw↑		896 vw 892 vw		898 ms, D?	896 s 890 vw, sh	ν_{26}
830				825 vw 810 s			810 vw, sh	
826 vs, A	831 w↓ 820 s↓	826 s↓ 820 vs↓		807 vw, sh				
822	816 s↑ 810 w↑	818 vs↑ 808 vvw	809 vs	801 s	824 vs	808 vs, P	803 s	ν_{14}
819	804 vvw							
				793 vvw			787 vvw	$\nu_{17} + \nu_{15}$
		785 vvw↓ 781 vw↓						
778c vw, B?	780 vvw↓ 774 vw↑	778 vw↑	780 vw, sh	777 s		782 vw, D	779 vw	ν_{28}
706	705 m↓	707 m↓		701 w, sh				
700 m, A	700 s↑	702 s↑	698 vs	698 m	701 s	700 vs, P	701 vs	ν_{18}
695				694 w, sh				
			675 w, sh	*	~676 vvw?		*	$\nu_{18}?$
	626 vvw	635 vvw						$\nu_{18} + \nu_{18}$
	612 vvw		621 w	610 vvw		619 vw	613 vvw	$2 \times \nu_{17}$
	590 vvw	594 vvw 568 vvw				592 vvw 561 vvw	560 vvw	$\nu_{17} + \nu_{30}$
555								
549 vw, A	548 vw↓		535 w	*	546 w↑	538 w, P↑	*	$\nu_{16}?$
543								
					525 vvw			
492	483 w↓							
486 m, A	486 m↑	486 m	484 m	483 m	486 s	485 s, P	484 ms 478 w, sh	ν_{16}
481								
					457 vvw			
307	305 w, sh↓	304 mw↓		300 w, sh			316 vw, sh	
302 w, A	299 mw↑	302 mw↑	297 m	298 mw	301 vs	301 vs, P	303 vs	ν_{17}
296								
			278 w	*?				$\nu_{17}?$
252								
248c vw, B	~253 vw	~251 vw	248 w	260 w	248 vw?	255 mw, D	255 mw	ν_{30}
243								
					150 w 137 w	164 w, P	175 mw	ν_{18}
							77 m	l.m.
							60 mw	l.m.
							45 w, sh	l.m.
							30 s	l.m.

* Abbreviations as in Table 1.
 † IR liquid data are from Ref. 3.

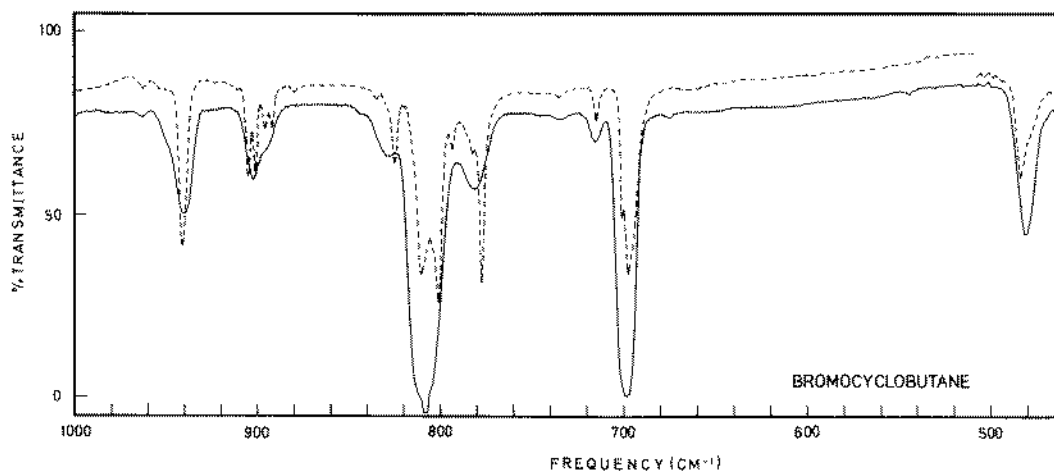


Figure 7. Infrared spectrum of bromocyclobutane at 90 K. Solid line, amorphous; dashed line, crystalline solid.

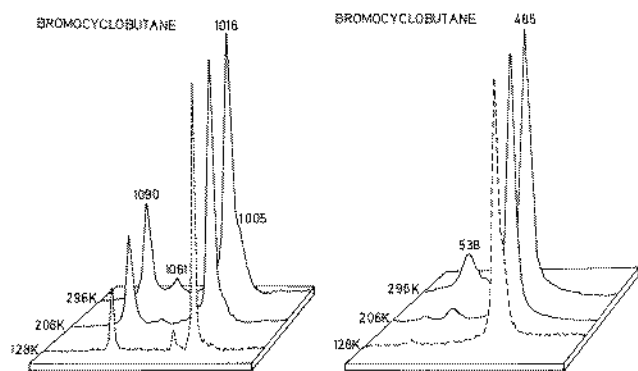


Figure 8. Raman curves of significant regions of bromocyclobutane. Solid lines, liquid at 296 and 206 K; dashed line, crystalline solid at 128 K.

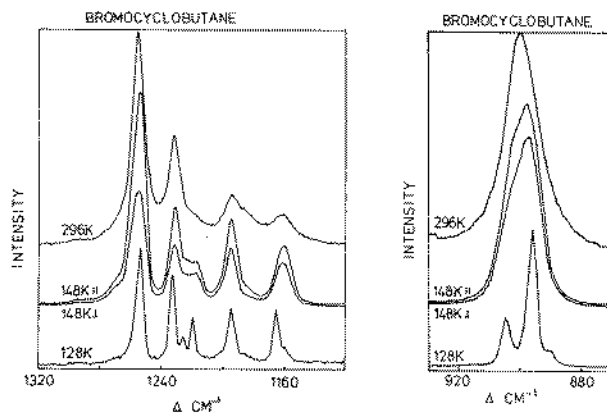


Figure 9. Raman spectra of the regions 1320–1120 and 930–870 cm^{-1} of bromocyclobutane as a liquid at 296 and at 148 K (with two polarization directions) and as a crystalline solid at 128 K.

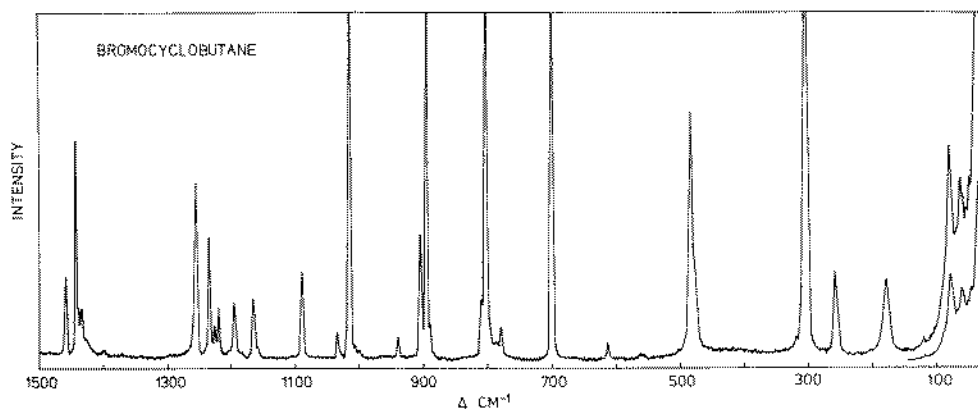


Figure 10. Raman spectrum of bromocyclobutane as a crystalline solid at 140 K.

being due to a multiple trapping site in the one matrix. However, when the same band is seen in both matrices, either the coincidence must be invoked that bands at the same frequency are appearing in both matrices because of multiple trapping sites or the band is explainable as an overtone or combination band. (Difference bands can obviously be ignored because of the low population of excited states at the temperature of measurement.) In many, but not all, cases of the multiple bands seen, plausible interpretations as overtones or combinations can easily be made.

When the thermal decomposition of chlorocyclobutane over the range 667–776 K was investigated, it was found to decompose by two pathways to ethylene and butadiene.²² Extrapolating these data to 900 K and adding together the two rate constants, we find that it would require approximately 3×10^{-3} s for 1% decomposition at that temperature. Since the actual time during which the compound is at the elevated temperature is more than an order of magnitude less than this, it is reasonable that we found no evidence of decomposition.

Likewise, the unimolecular decomposition²³ of bromocyclobutane from 791 to 1224 K has been studied. Extrapolating the data downward to 700 K gives a half-life at that temperature of 300 s. Obviously, no observable decomposition should be expected.

High-pressure crystal

The crystals formed at high pressure gave spectra similar to those found at low temperature. 'Pressure annealing' of chloro- and bromo-cyclobutane to produce a single crystal did not significantly change their spectra. A very weak IR band at 779 cm^{-1} in the liquid spectrum of chlorocyclobutane was strongly enhanced in both the high-pressure and low-temperature crystal spectra. Otherwise, with the exception of some smaller alterations in intensity and the usual shifts with pressure toward higher frequency, the spectra were much like those of the crystal which has been reported earlier. Specifically, the bands ascribed by Rothschild¹ to the C–X stretch of the axial conformer disappeared. From the close similarity of the spectra to those of the liquid, it is obvious that the conformer crystallizing at high pressure in each case is the equatorial one.

Raman low-temperature crystal spectra

In the Raman experiments in which the samples were crystallized from the melt, we have found convincing evidence showing that chloro- and bromo-cyclobutane exist as a mixture of two conformers.

In chlorocyclobutane we note vanishing peaks at

1080, 1014, 678 and 351 cm^{-1} (vapour values), in addition to the clear 630 cm^{-1} band observed by Rothschild.¹ Moreover, the variable-temperature spectra revealed that all these Raman bands were enhanced with temperature in the liquid, as shown in Figs 3–5 for the bands at 1080, 1012, 680, 618 and 352 cm^{-1} (liquid values). Therefore, it seems clear that all these bands are due to the axial conformer present in very low concentration (<5%) at these temperatures.

In bromocyclobutane we have detected Raman bands at 1063 and 1005 cm^{-1} (vapour) which are enhanced with temperature in the liquid spectra and vanish in the crystal. In addition, there are uncertain bands at 675 and 278 cm^{-1} which may be axial fundamentals in addition to the band at 546 cm^{-1} reported previously.¹

Infrared low-temperature crystal spectra

With the observed changes in the Raman spectra in mind, we can see how these changes agree with what can be observed in the infrared crystallization.

In chlorocyclobutane the band at 616 cm^{-1} clearly disappears.¹ Likewise, the bands at 1080, 678 and 352 cm^{-1} vanished on crystallization. The infrared band at 1018 cm^{-1} is asymmetric in the liquid with a 'bulge' around 1010 cm^{-1} on the low-frequency side. It becomes much more symmetrical in the crystal as the low-frequency bulge vanishes. No additional disappearing peaks could be added to those obtained from the Raman spectrum.

In bromocyclobutane the bands³ at 1001, 675, 535 and possibly 278 cm^{-1} disappear in the IR spectrum on crystallization, in good agreement with the results from the Raman spectra (see above).

General comments

We have long been dissatisfied with any explanations in favour of two conformers which rely on the idea that only one vibrational frequency changes substantially between the two conformers. To our knowledge, no other such cases are known. With a total of five bands which differ between the two conformers in chlorocyclobutane and four or possibly five in bromocyclobutane, we think we have met our own objection. More important is that in looking at the intensities of these bands relative to their counterparts which lie near them, we can comment on just how weak they are. The most intense of the five Raman bands in chlorocyclobutane at 618 is about 7% as intense as the band at 528 cm^{-1} . However, the band at 680 cm^{-1} is only about 1.3% as intense as the band at 717, and the band at 1080 cm^{-1} is approximately 3.6% as intense as that at 1102 cm^{-1} . Thus, given the usual experience that we can detect conformers only when their abundance is at least 5%, the long delay in finding confirming evidence for the second conformer becomes more understandable. This is clearly a case in which there is only 3–4% of the second conformer.

At this juncture it is also useful to refer back to the matrix spectra to point out that none of the bands in question appears in either the argon or nitrogen matrix spectra. This is completely consistent with our interpretation of them as belonging to a second conformer

which disappears as the matrices are formed. Any explanation of them as being due to impurities will have great difficulties with this fact.

Energy difference between conformers

From his electron diffraction study of chlorocyclobutane, Jonvik¹¹ estimated ΔH° (axial–equatorial) to be 6 or 4 kJ mol^{-1} (based on two different assumptions) in the vapour. Our own values, obtained from Raman spectra of the vapour in the range 295–334 K, gave a value of $\Delta H^\circ = 5.2 \pm 1.9\text{ kJ mol}^{-1}$, whereas a liquid value of $5.7 \pm 0.7\text{ kJ mol}^{-1}$ was calculated from spectra recorded in a much wider temperature range (205–345 K).

For bromocyclobutane, ΔH° (axial–equatorial) values of 9 and 7 kJ mol^{-1} (different assumptions) were obtained from gaseous electron diffraction.¹¹ Measurements of IR vapour-phase intensities between 303 and 444 K gave 4 kJ mol^{-1} , whereas liquid-phase measurements between 262 and 173 K gave²⁴ 5.3 kJ mol^{-1} . We obtained $\Delta H^\circ = 8.2 \pm 1.2\text{ kJ mol}^{-1}$ in the vapour (299–330 K) and $9.0 \pm 0.5\text{ kJ mol}^{-1}$ in the liquid (172–343 K). Obviously, the liquid-state values, which were based on a much wider temperature range and better signal-to-noise ratio, are more reliable than the vapour-phase values. Hence it is uncertain if the ΔH° values of the vapour and liquid states are different. Because of the low barrier to ring conversion in these molecules, the axial conformer could not be trapped at 17 K. Hence the much more reliable hot nozzle matrix isolation method,²⁵ covering a typical temperature range of 300–900 K, could not be employed for these compounds.

A lower limit of 1.5 kJ mol^{-1} for the barrier between the axial and equatorial conformers for both compounds was estimated from the electron diffraction results.¹¹ From our matrix isolation experiments we can give a higher limit of 5 kJ mol^{-1} for the barrier in both molecules when trapped in both argon and nitrogen matrices. It may be mentioned that both cyanocyclobutane and 1-chloro-1-fluorocyclobutane also have barriers lower than 5 kJ mol^{-1} in argon and nitrogen matrices. In 1-chloro-1,2,2-trifluorocyclobutane and 1,1,2-trichloro-2,3,3-trifluorocyclobutane¹⁹ both conformers were trapped in the matrices and annealing experiments implied barriers of ca. 7 kJ mol^{-1} for both compounds, as reported in a preliminary communication.²⁶

Spectral assignments

The vibrational spectra of chloro- and bromocyclobutane were reported by Rothschild¹ and later by Durig and co-workers^{2,3} who also included various deuterated species. The assignments of these authors are generally in good agreement, and we shall only comment the instances where our interpretations differ from theirs.^{1–3} Our assignments are listed in Tables 1 (chlorocyclobutane) and 2 (bromocyclobutane), and the fundamentals below 1400 cm^{-1} are given in Tables 3 and 4 together with the results of the force constant calculations.

Table 3. Observed and calculated frequencies for chlorocyclobutane

ν_i	Equatorial		PFD ^b	Axial		$\nu(\text{eq.}) - \nu(\text{ax.})$	
	Obs. ^a	Calc.		Obs.	Calc.	Obs.	Calc.
8	1286	1313	16 $\alpha\text{CH}\delta$, 36 βCH_2 wa, 18 ring st		1324		-11
9	1227	1255	32 βCH_2 wa, 24 βCH_2 tw, 15 $\alpha\text{CH}\delta$		1268		-13
10	1206	1218	48 βCH_2 tw, 14 γCH_2 ro, 12 βCH_2 wa		1217		1
11	1106	1101	48 ring st (breath)	1080	1046	26	55
12	1022	966	10 βCH_2 ro, 44 rings st, 10 ring δ	1014	917	8	49
13	912	886	38 ring st, 23 ring δ , 8 βCH_2 ro		890		-4
14	848	869	12 ring δ , 49 $\alpha\text{CH}\delta$, 17 γCH_2 ro		863		6
15	717	700	44 γCH_2 ro, 13 CCl st, 10 ring st	677	661	40	39
16	530	531	23 CCl st, 43 ring δ , 26 βCH_2 ro	630	635	-100	-104
17	370	371	53 CCl δ , 32 CCl st	355	369	15	2
18	156	156	121 ring pucker, 43 β , γCH_2 ro		142		14
22	1264	1262	64 γCH_2 wa, 24 βCH_2 wa		1269		-7
23	1239	1229	16 βCH_2 wa, 16 γCH_2 tw, 36 $\alpha\text{CH}\delta$		1260		-31
24	1222	1207	33 γCH_2 tw, 24 βCH_2 tw, 22 βCH_2 wa		1212		-5
25	1164	1189	23 $\alpha\text{CH}\delta$, 34 ring st, 30 βCH_2 wa		1183		6
26	1031	1029	70 βCH_2 tw, 23 γCH_2 tw		1031		-2
27	938	926	72 ring st		948		-22
28	904	907	58 ring st, 31 $\alpha\text{CH}\delta$		895		12
29	781	768	92 βCH_2 ro		760		8
30	283	283	90 CCl δ		280		3

^a Vapour- or liquid-phase values. Fundamentals above 1400 cm^{-1} have been omitted.

^b Potential energy distribution defined as $X_{ik} = 100F_{ik} L_{ik}^2/\lambda_k$. a, Antisymmetric; s, symmetric; st, stretch; δ , deformation; r, rock; w, wag; tw, twist; sc, scissor; α , β and γ denote carbon positions in the ring. Adjusted force constants: CCl st 3.182 mdyn \AA^{-1} , CCl δ in-plane 1.870 mdyn \AA rad^{-2} , CCl δ out-of-plane 0.879 mdyn \AA rad^{-2} , ring puckering 0.175 mdyn \AA rad^{-2} .

Table 4. Observed and calculated frequencies for bromocyclobutane

ν_i	Equatorial		PED ^b	Axial		$\nu(\text{eq.}) - \nu(\text{ax.})$	
	Obs. ^a	Calc.		Obs.	Calc.	Obs.	Calc.
8	1262	1300	48 βCH_2 wa, 22 ring st, 11 $\alpha\text{CH}\delta$		1307		-7
9	1234	1246	21 $\alpha\text{CH}\delta$, 20 βCH_2 wa, 18 βCH_2 tw		1263		-17
10	1198	1217	52 βCH_2 tw, 13 γCH_2 ro, 12 βCH_2 wa		1217		0
11	1092	1092	54 ring st (breath)	1063	1041	29	51
12	1016	962	10 βCH_2 ro, 44 ring st, 10 ring δ	1006	915	10	47
13	908	886	40 ring st, 23 ring δ , 8 βCH_2 ro		888		-2
14	826	865	15 ring δ , 19 γCH_2 ro, 43 $\alpha\text{CH}\delta$		859		6
15	700	685	46 γCH_2 ro, 15 ring δ , 12 βCH_2 ro	676	646	24	39
16	486	497	21 CBr st, 33 ring δ , 24 βCH_2 ro	549	592	-63	-95
17	302	299	39 CBr δ , 45 CBr st		305		-6
18	150	150	117 ring pucker, 40 β , γCH_2 ro		133		17
22	1282	1262	64 γCH_2 wa, 24 βCH_2 wa		1268		-6
23	1226	1227	16 βCH_2 wa, 20 γCH_2 tw, 33 $\alpha\text{CH}\delta$		1260		-33
24	1219	1206	29 γCH_2 tw, 28 βCH_2 wa, 22 βCH_2 tw		1211		-5
25	1159	1189	26 $\alpha\text{CH}\delta$, 32 ring st, 26 βCH_2 wa		1182		-7
26	1029	1029	70 βCH_2 tw, 23 γCH_2 tw		1030		-1
27	938	926	72 ring st		946		-20
28	898	903	60 ring st, 30 $\alpha\text{CH}\delta$		894		9
29	778	767	92 βCH_2 ro, 17 γCH_2 tw		760		7
30	248	248	91 CBr δ		246		2

^a Vapour- or liquid-phase values. Fundamentals above 1400 cm^{-1} have been omitted.

^b Potential energy distribution defined as $X_{ik} = 100F_{ik} L_{ik}^2/\lambda_k$. a, Antisymmetric; s, symmetric; st, stretch; δ , deformation; r, rock; w, wag; tw, twist; sc, scissor; α , β , γ denote carbon positions in the ring. Adjusted force constants: CBr st 2.780 mdyn \AA^{-1} , CBr δ in-plane 1.773 mdyn \AA rad^{-2} , CBr δ out-of-plane 0.796 mdyn \AA rad^{-2} , ring puckering 0.175 mdyn \AA rad^{-2} .

In the region 1300–1150 cm^{-1} we observed for chlorocyclobutane Raman bands at 1281, 1260, 1238, 1227, 1219, 1204 and 1166 cm^{-1} in a cooled liquid at 150 K, and all of these bands were also present in the IR and Raman crystal spectra. The two bands at 1227 and 1219 cm^{-1} , prominent at 150 K, were covered by neighbouring bands at ambient temperature and were not detected by the earlier workers.^{1–3} All these seven bands are assigned as equatorial fundamentals (Tables 1 and 3). A medium-intensity band reported at 1123 cm^{-1} and assigned² as ν_{25} was not observed by us or by Rothschild¹ and must be caused by an impurity.

As mentioned, the 1080 cm^{-1} band is clearly an axial fundamental ν'_{11} , but was previously interpreted^{1,2} as an equatorial combination band. IR and Raman bands around 1032 cm^{-1} , not reported previously,^{1,2} were observed by us in various spectra as a shoulder on the intense band at 1020 cm^{-1} and assigned as ν_{26} . The Raman bands at 1014 (vapour) and 1012 cm^{-1} (cooled liquid), enhanced with temperature, are absent in the crystal and assigned as ν'_{12} of the axial conformer. An IR liquid band at 971 cm^{-1} assigned² as ν_{26} also observed by Rothschild¹ was not detected by us and is considered to be an impurity band.

A broad Raman band at 902 cm^{-1} previously assigned^{1,2} as an a'' fundamental shows a distinct shoulder at 906 cm^{-1} in the cooled liquid and also in the crystal and was assigned by us as ν_{13} . Two Q -branches at 850 and 846 cm^{-1} in IR were interpreted² as being due to two fundamentals ν_{13} and ν_{14} . However, only one Q -branch at 849 cm^{-1} was observed in the Raman vapour spectrum. Although two peaks at 843 (vs) and 838 (w) cm^{-1} were observed in the nitrogen matrix, they completely changed intensities after annealing and the second peak was apparently caused by a matrix effect. Therefore, we have only assigned one fundamental (ν_{14}) to this band. A band at 815 cm^{-1} reported in the IR liquid and argon matrix spectra and assigned² as ν_{29} was not seen in our spectra, except as uncertain peaks in the crystal spectra, and was interpreted as a combination band.

As mentioned above, the 680 cm^{-1} bands are interpreted as an axial fundamental ν'_{15} rather than a combination band,^{1,2} whereas the 630 cm^{-1} band is the most prominent axial band.^{1,2} Surprisingly, Kalasinsky *et al.*²⁷ recently listed the 630 cm^{-1} band as equatorial in a survey table of eight monosubstituted cyclobutanes. Finally, the bands at 352 cm^{-1} are assigned as the axial fundamental ν'_{17} rather than as an overtone.²

The IR and Raman spectra of bromocyclobutane are very similar to those of chlorocyclobutane, and the spectral interpretations will be described very briefly. Durig and Green³ interpreted the out-of-plane CH bending at 963 (a'') and the in-plane CH bending at 1262 cm^{-1} (a'). Our force-constant calculations strongly suggested that both these modes should be situated in the region 1300–1150 cm^{-1} , in agreement with force constant calculations on 2-chloro-²⁸ and 2-bromopropane.²⁹ Therefore, seven fundamentals (three a' and four a'') were assigned in the region 1300–1150 cm^{-1} for both bromo- and chloro-cyclobutane (see above). The bands at 1063 and 1006 cm^{-1} were ascribed to the axial fundamentals ν'_{11} and ν'_{12} , interpreted as equatorial combination bands or impurity bands by the earlier workers.^{1,3}

The 898 cm^{-1} band, which seems depolarized, clearly has a polarized shoulder at 908 cm^{-1} readily seen in the cooled liquid (Fig. 9), in perfect agreement with the bands at 902 and 906 cm^{-1} in chlorocyclobutane. They are interpreted as ν_{28} and ν_{13} in both spectra. The uncertain band at 675 cm^{-1} is interpreted with some doubt as the axial mode ν'_{15} for bromocyclobutane, corresponding to the band at 680 cm^{-1} in chlorocyclobutane. The axial C–Br stretch ν'_{16} at 538 cm^{-1} agrees with the results of the earlier workers,^{1,3} whereas the axial mode ν'_{17} at 278 cm^{-1} is uncertain. It is not surprising that the axial bands are harder to verify in bromocyclobutane than in chlorocyclobutane since ΔH° and apparently also ΔG° are more unfavourable in the former.

Force constant calculation

The scaled *ab initio* force field for cyclobutane derived by Bahnegyi *et al.*³⁰ was modified to fit chloro- and bromo-cyclobutane. In their symmetry force field, containing 73 independent parameters, one complete set of force constants for CH stretch, CH_2 scissor, CH_2 wag, CH_2 twist and CH_2 rock were removed. Instead, we introduced diagonal force constants for C–X stretch, CCH in-plane and out-of-plane bend and CCX in-plane and out-of-plane bend, transferred from secondary chlorides³¹ and bromides.²⁸ While all the remaining *ab initio* force constants were kept constant, three (C–X stretch and CCX bend) force constants were adjusted by a least-squares program to the equatorial fundamentals of chloro- and bromo-cyclobutane using the adopted³⁰ geometry for the cyclobutane with $r(\text{C–Cl}) = 179.5$ and $r(\text{C–Br}) = 194$ pm. Subsequently, the same force constants were employed to calculate the axial conformer bands as listed in Tables 3 and 4 for chloro- and bromo-cyclobutane, respectively. For the sake of brevity, only the fundamentals below 1400 cm^{-1} are given. Considering the lack of interaction terms for the C–X stretch and the CCH and CCX in-plane and out-of-plane bending, the agreement between the observed and calculated wavenumbers are satisfactory in most cases.

The calculations support the assumption of three a' and four a'' modes situated between 1300 and 1150 cm^{-1} for both compounds. The fundamentals ν_{11} , ν_{12} , ν_{15} and ν_{16} are those which are seen as separate bands for the axial conformer in both compounds (possibly with ν_{17} in addition for chlorocyclobutane). It is interesting that with our present force field these a' modes have the largest calculated shifts between the axial and equatorial conformers, as seen in Table 3 for chlorocyclobutane and in Table 4 for bromocyclobutane.

Acknowledgements

The authors are grateful to A. Horn and J. Invaco for technical help. Financial support was provided by the Research Corporation, the Norwegian Marshall Fund, NAVF and NTNF.

REFERENCES

1. W. G. Rothschild, *J. Chem. Phys.* **45**, 1214 and 3599 (1967).
2. J. R. Durig and A. C. Morrissey, *J. Chem. Phys.* **46**, 4854 (1967).
3. J. R. Durig and W. H. Green, *J. Chem. Phys.* **47**, 673 (1967).
4. C. S. Blackwell, L. A. Carreira, J. R. Durig, J. M. Karriker and R. C. Lord, *J. Chem. Phys.* **56**, 1706 (1972).
5. J. R. Durig, A. C. Shing and L. A. Carreira, *J. Mol. Struct.* **17**, 423 (1973).
6. H. Kim and W. D. Gwinn, *J. Chem. Phys.* **44**, 865 (1966).
7. W. G. Rothschild and B. P. Dailey, *J. Chem. Phys.* **36**, 2931 (1962).
8. M. Y. Fong and M. D. Harmony, *J. Chem. Phys.* **58**, 4260 (1973).
9. J. R. Durig, L. A. Carreira and W. J. Lafferty, *J. Mol. Spectrosc.* **46**, 187 (1973).
10. (a) W. Caminati, B. Velino and R. G. D. Valle, *J. Mol. Spectrosc.* **129**, 284 (1988). (b) M. Dakkouri, K. Ruedel, V. Typke and W. Caminati, *Acta Chem. Scand. Ser. A*, **42**, 519 (1988). (Added in proof.)
11. T. Jonvik, *J. Mol. Struct.* **172**, 213 (1988); Dissertation, Oslo (1986).
12. T. Jonvik and J. E. Boggs, *J. Mol. Struct. (THEOCHEM)* **85**, 293 (1981).
13. J. R. Durig, T. J. Geyer, T. S. Little and M. Dakkouri, *J. Phys. Chem.* **89**, 4307 (1985).
14. J. R. Durig, T. J. Geyer, T. S. Little and V. F. Kalasinsky, *J. Phys. Chem.* **86**, 545 (1987).
15. M. Dakkouri and H. Oberhammer, *J. Mol. Struct.* **102**, 315 (1983).
16. M. Dakkouri, *J. Mol. Struct.* **103**, 289 (1985).
17. A. C. Legon, *Chem. Rev.* **80**, 231 (1980).
18. F. H. Allen, *Acta Crystallogr. Sect. B* **40**, 64 (1984).
19. D. L. Powell and P. Klaeboe, *Acta Chem. Scand., Ser. A* **32**, 71 (1978).
20. F. A. Miller and B. M. Harney, *Appl. Spectrosc.* **24**, 291 (1970).
21. J. E. Gustavsen, P. Klaeboe and H. Kvila, *Acta Chem. Scand. Ser. A* **32**, 285 (1976).
22. A. T. Cocks and H. M. Frey, *J. Am. Chem. Soc.* **91**, 7583 (1969).
23. K. D. King and R. G. Gilbert, *Int. J. Chem. Kinet.* **12**, 339 (1980).
24. V. T. Aleksanyan, S. V. Zotova and M. G. Ezernitskaya, *Zh. Strukt. Khim.* **14**, 1110 (1973).
25. G. O. Braathen, A. Gatial and P. Klaeboe, *J. Mol. Struct.* **157**, 73 (1987).
26. D. L. Powell, A. Gatial, P. Klaeboe, C. J. Nielsen and A. J. Kondow, *J. Mol. Struct.* **173**, 389 (1988).
27. V. F. Kalasinsky, W. C. Harris, P. C. Holtzclaw, T. S. Little, T. J. Geyer and J. R. Durig, *J. Raman Spectrosc.* **18**, 581 (1987).
28. T. Sundius, *J. Mol. Spectrosc.* **64**, 47 (1977).
29. R. G. Snyder, *J. Mol. Spectrosc.* **28**, 273 (1968).
30. G. Bahnegyi, G. Fogarasi and P. Pulay, *J. Mol. Struct. (THEOCHEM)* **89**, 1 (1982).
31. W. H. More and S. Krimm, *Spectrochim. Acta, Part A* **29**, 2025 (1973).